ELSEVIER

Journal of Photochemistry and Photobiology B: Biology 62 (2001) 1–8

Journal of Photochemistry and Photobiology B:Biology

www.elsevier.com/locate/jphotobiol

Modeling the effects of ultraviolet radiation on estuarine phytoplankton production: impact of variations in exposure and sensitivity to inhibition

Patrick J. Neale

Smithsonian Environmental Research Center, Edgewater, MD 21037, USA

Received 11 November 2000; accepted 7 June 2001

Abstract

Spectral ultraviolet (UV) irradiance, water column attenuation and biological weighting functions for inhibition of phytoplankton photosynthesis have been measured for the Rhode River, a subestuary of the Chesapeake Bay. Together, these measurements can be used to estimate UV effects on water column production, but each factor shows a significant range of variability even just considering summer time conditions. A sensitivity analysis of UV inhibition is described which assesses the effect of this variation for different combinations of 28 irradiance spectra, 8 biological weighting functions (BWFs) and 16 water column irradiance profiles. Over all combinations, production averaged about 84% relative to potential production in the absence of UV effects. For a few combinations, relative production was as low as 67%, or as high as 97%, but for most combinations the range was 75–95%. Variations in the sensitivity of the phytoplankton assemblage, i.e. the BWF, and optical properties, represented by a transparency ratio of biologically effective UV to photosynthetically available radiation (PAR), had large effects on water column production. A simple relationship for UV inhibition of water column production is developed based on inhibition at the surface and the ratio of UV and PAR transparency.

Keywords: Biological weighting functions; Photoinhibition; UV-B; UV-A

1. Introduction

Ultraviolet radiation (UV, 280–400 nm) is increasingly recognized as a potent influence on biological and chemical processes in the aquatic environment [1–3]. In part, this recognitions stems from concerns about the effect of stratospheric ozone loss, which results in a wavelength-dependent increase in incident UV-B (280–320 nm, with 290 nm the lower bound for solar irradiance) [4]. This depletion is caused by the breakdown of anthropogenic chlorofluorocarbons (CFCs) in the stratosphere. The release of CFCs is now limited by the Montreal Protocol. Nevertheless ozone depletion continues, apparently due to the cooling of the stratosphere which accompanies 'greenhouse gas' induced surface warming [5].

There are also strong ecological effects of the long-wavelength, solar UV-A (320–400 nm). Indeed, inhibition of phytoplankton photosynthesis by solar UV-A is generally greater than inhibition by solar UV-B [6,7]. Many environmental changes affect UV exposure over the full waveband. Transmission of UV in aquatic environments is affected by variations in dissolved organic compounds and suspended particulates. Such variation is more important than ozone depletion in determining UV exposure in the water column of lakes [8–10]. Full band incident UV is also affected by a number of variables that are vulnerable to anthropogenic and natural variation, such as cloud cover and atmospheric aerosols [11].

The importance of variations in the UV climate to chemical and biological processes in aquatic environments can be assessed by application of spectral weighting functions. Biological weighting functions (BWFs) describe the effectiveness of radiation of different wavelengths to produce a biological response, such as inhibition of photosynthesis. A wavelength-dependent description of UV effects on photosynthesis (BWF/P-I model) has been developed, which describes photosynthesis as a function of photosynthetically available radiation (PAR) and photoinhibition as a function of both PAR and UV [6,12]. The model is fit using laboratory measurements of photosynthesis under filtered solar-simulator (xenon arc) irradiance [6,12]. The predictions of the model agree with the results of solar incubations in Antarctica [13] and in situ productivity profiles in lakes [14]. Using this con-

E-mail address: neale@serc.si.edu (P.J. Neale).

1011-1344/01/$ – see front matter
PII: S1011-1344(01)00159-2

ceptual approach, BWFs have been measured for diverse phytoplankton, including cultures [6,15] and natural assemblages in Antarctica [12,16] and a shallow subestuary of the Chesapeake Bay [17]. These studies have revealed more than ten-fold variation in the sensitivity of phytoplankton photosynthesis to UV inhibition.

Among the issues that can be addressed using spectral weighting functions is the relative importance of variations in environmental factors versus sensitivity to UV in enhancing or ameliorating the effects of UV in aquatic ecosystems. A modeling analysis of an Antarctic ecosystem (Weddell-Scotia Confluence, WSC) showed that both physiological variability (i.e. BWFs) and variation in exposure, related to changes in the depth of vertical mixing, can profoundly affect predicted inhibition of water column photosynthesis [18]. The effect of ozone depletion was significant but secondary to these other factors. The relative importance of variation in irradiance and sensitivity has not been modeled in other aquatic environments.

This report describes the results of an initial sensitivity analysis of factors affecting UV inhibition of water column photosynthesis in the Rhode River, which is a turbid, eutrophic [19] subestuary on the western shore of the Chesapeake Bay in Maryland, USA. The Smithsonian Environmental Research Center, located adjacent to the Rhode River, is a long-term monitoring site for solar spectral UV-B [20]. The BWFs for phytoplankton assemblages in the Rhode River were measured on a monthly basis during 1995 and 1996 [17]. More recently, the Rhode River has been regularly sampled for spectral attenuation [21]. In this report, we make an initial evaluation of the relative importance of variation in BWFs, solar UV and water transparency in modifying the predicted effect of UV on summertime water column production.

2. Methods

2.1. Input data

The primary sampling site is the Rhode River Station 4B, which is located in an estuary segment with a mean depth of 1.6 m [22]. Sampling and experimental determination of the BWFs using the photoinhibition approach has been previously described [17]. Profiles of spectral irradiance ($E_d(\lambda,z)$, mW m^{-2} nm^{-1}) were measured using a Satlantic OCP 200 radiometer with filter center wavelengths of 325, 340, 380 nm (2 nm bandwidth) and ten wavelengths in the visible range (10 nm bandwidth). Incident spectral UV-B irradiance (mW m^{-2} nm^{-1}, 1 min averages) is continuously measured at SERC over the spectral range of 290–325 nm using a multifilter radiometer (SR18) with eighteen 2-nm bandwidth filters [23].

Model estimates of clear sky, solar noon spectral irradiance (290–700 nm) were obtained using a radiative transfer model [24] as implemented by the STAR software package (H. Schwander, University of Munich).

2.2. Sensitivity analysis

The analysis focused on early summer conditions as UV exposure is highest during this period. Accordingly, a 1–2-month period of observations was selected, with the period centered around summer solstice. The selected data included 28 days of irradiance measurements (June 7–July 5, 1999), 8 BWFs (May 3–July 27, 1995 and 1996) and 16 profiles of downwelling spectral irradiance (June 6–August 6, 1999). The BWFs were measured in a different year to the irradiance data, however conditions were generally the same between the two summers. Moreover, the BWFs showed no significant correlation with irradiance data and proxy indicators of water column transparency measured during 1995 and 1996 [17]. Variations in spectral transparency of the Rhode River and incident solar irradiance also were not correlated during the period of study (data not shown). Therefore, to a first approximation, variations in each measurement over this period were considered statistically independent.

The general approach for the sensitivity analysis was to calculate midday, integral water-column photosynthesis over surface to 1.6 m depth for each combination of measured irradiance, BWF and spectral attenuation. The BWF/P-I was used to calculate photosynthesis as a function of depth ($P^B(z)$, mg C mg Chl^{-1} h^{-1})

$$P^B(z) = P_s^B \tanh\left(E_{PAR}(z)/E_s\right) \cdot \left(\frac{1}{1 + E^*_{inh}(z)}\right) \quad (1)$$

where P_s^B is the maximum attainable rate of photosynthesis in the absence of photoinhibition; $E_{PAR}(z)$ is PAR expressed as irradiance in energy units (W m^{-2}) and is determined by the attenuation coefficient for PAR (K_{PAR}, m^{-1}) using the expression $E_{PAR}(0)\exp(-K_{PAR}z)$; E_s is a saturation parameter for photosynthesis. The inhibition term is a function of UV spectral irradiance ($E(\lambda,z)$, mW m^{-2} nm^{-1}) expressed as biologically-weighted exposure, $E^*_{inh}(z)$ (dimensionless), where

$$E^*_{inh}(z) = \sum_{\lambda=290nm}^{395\ nm} \epsilon(\lambda) \cdot E(\lambda,z) \cdot \Delta\lambda \quad (2)$$

$\epsilon(\lambda)$ is the wavelength-dependent biological effectiveness (i.e. the BWF) for inhibition of photosynthesis by UV (mW $m^{-2})^{-1}$. Although a parameter for E_{PAR} dependent inhibition (i.e. ϵ_{PAR}) can be included in Eq. (2), it was not needed [17]. The BWF/P-I model (Eq. (1)) is similar to that described by Cullen and Neale [25], except that potential photosynthesis is described by a hyperbolic tangent $P-E$ function [26]. For convenience of comparison, water-column photosynthesis (P_z, mg C m^{-2} h^{-1}) was calculated for unit P_s^B and chlorophyll concentration

(1 mg Chl m^{-3}) by evaluating $P^B(z)$ at 0.1 m intervals from 0 to 1.6 m and integrating over depth. During the observation period, P_s^B actually varied from 3 to 18 mg C mg Chl^{-1} h^{-1} and Chl varied from 15 to 45 mg Chl m^{-3}. For comparison, 'potential' water column photosynthesis in absence of UV effects (P_{zpot}, mg C m^{-2} h^{-1}) was calculated the same way except that $E^*_{inh}(z)$ was set to 0.

Evaluation of the weighted irradiance requires full band spectral irradiance (290–700 nm) as function of depth. Incident spectral solar UV-B at the surface was measured by the SR18, these measurements were averaged for the one period around solar noon (1300 h local daylight savings time). Complete evaluation of weighted irradiance required extension of this spectrum to the 325–400 nm spectral region not measured by the SR18 which was made by reference to model spectra calculated using the STAR program. Program inputs were as follows: measurement date and time, i.e. solar noon (1700 h UTC at SERC location), 'continental polluted air' for aerosol type, summer ozone profile, total column ozone as estimated from TOMS (toms.gsfc.nasa.gov) and observed barometric pressure. The modeled spectra (smoothed using a 2-nm bandwidth gaussian filter) was very similar to the SR18 measurements under clear sky conditions (Fig. 1). The UV-A spectrum (325–400 nm, at 1-nm intervals) was then estimated by applying a constant factor to the model spectra for each day based on the proportion between observed and modeled spectra over 320–322 nm. Integral PAR (400–700 nm) irradiance was calculated using the same proportion. Clear sky conditions were prevalent during the period: two-thirds of the measurements were within 20% of modeled irradiance at 320 nm (Fig. 2a). Cloudy conditions typically resulted in a reduction to about 30% of clear sky irradiance (Fig. 2a).

Attenuation coefficients were calculated from depth profiles of spectral irradiance and used to estimate in situ spectral irradiance at 10-cm intervals between 0 and 1.6 m, after correcting for surface reflection (see [18]). Spectral attenuation coefficients for wavelengths of the irradiance data (SR18 wavelengths in UV-B and every nanometer in the UV-A) was obtained by fitting an exponential equation (i.e. linear regression on log transformed coefficients) to attenuation coefficients estimated at 325, 340, 380, 412, 510, 532 and 555 nm. Attenuation coefficients for $\lambda < 325$ nm were obtained by extrapolation of the fitted curve. Coefficients in this range may be underestimated if the spectral slope increases in the UV-B, as has been reported in other waters [27]. In all 16 attenuation spectra, the coefficient of determination (R^2) for the exponential equa-

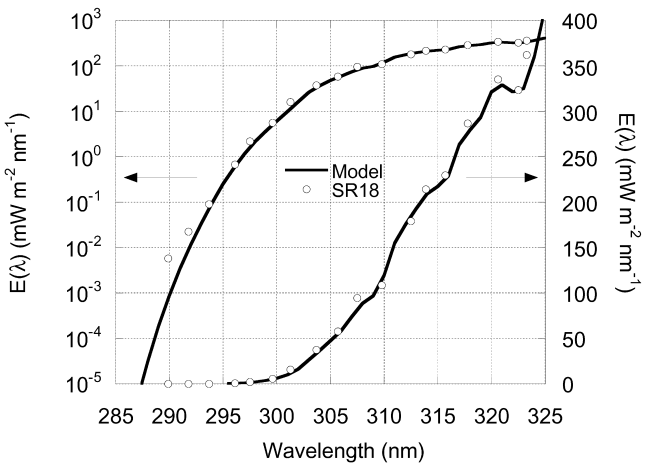

Fig. 1. Example of incident UV-B irradiance spectrum for the Rhode River as used in the calculation of water column production. Shown are spectra (mW m^{-2} nm^{-1}) obtained for midday, clear-sky conditions on June 20, 1999. Spectra were measured with the SR18 multifilter UV-B radiometer and averaged for the 1-h period centered around solar noon, with irradiance plotted at the filter center wavelength (circles). Each filter has a nominal bandwidth of 2 nm (FWHM). Spectra were also calculated using a radiative transfer model (line) as implemented by the STAR program using a 2-nm bandwidth, observed barometric pressure and total column ozone from TOMS. Spectra are plotted on both a logarithmic (left) and linear (right) scale.

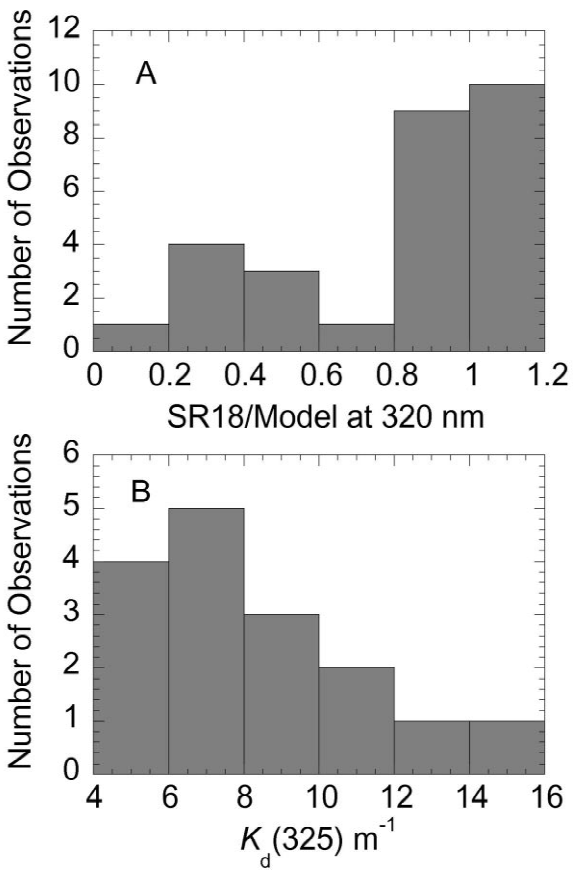

Fig. 2. Variation in factors affecting phytoplankton exposure to UV in the Rhode River. (A) Distribution of incident spectral irradiance at 320 nm for a 28-day period centered around June 21, 1999 as a proportion of the clear sky 320 nm irradiance calculated for each day using the STAR program (see Fig. 1). (B) Distribution of downwelling attenuation coefficient for spectral irradiance at 325 nm (K_d [325], m^{-1}) as calculated from 16 profiles of water-column irradiance in the Rhode River and adjacent waters of the Chesapeake Bay measured during the period June 6–August 6, 1999.

tion exceeded 0.98 ($P<10^{-6}$). Spectral attenuation at 325 nm was usually between 4 and 8 m^{-1}, but was occasionally as high as 15 m^{-1} (Fig. 2b). An overall attenuation coefficient for PAR (K_{PAR}, m^{-1}) was calculated from attenuation coefficients in the 400–700 nm range.

The eight selected BWFs spanned the middle range of variability for the Rhode River [17]. The range of variation between the most and least sensitive (as indicated by weight at 325 nm) was about 3-fold, with other weights evenly distributed between these extremes. This compares to an approximate 10-fold variation between minimum and maximum sensitivity overall [17]. Average weight at 325 nm is 1.22×10^{-4} (mW $m^{-2})^{-1}$. The coefficient of variation (S.E./mean) for the BWF coefficients is about 10%.

3. Results

Calculations of water-column production and related variables are summarized in Table 1. Midday productivity predicted by the model averages around 1 mg C m^{-2} h^{-1} (for unit Chl concentration and P_s^B) when UV effects are included, compared to potential production of about 1.2 mg C m^{-2} h^{-1} in the absence of UV. In other words, under the chosen model conditions UV modeled production was about 84% overall of potential production and UV inhibition is about 16%. Over all combinations of variables, the relative production ($P^*_z=P_z/P_{zpot}$) ranged from 67 to 97%, with most combinations lying in the range of 75–95% (Fig. 3b). The lowest relative production (severest inhibition) occurred with the most sensitive assemblages (July 3, 1996 and July 12, 1995) under clear sky conditions, whereas highest relative production (least inhibition) occurred in combinations of the least sensitive assemblage (June 17, 1995) under cloudy conditions [$E(\lambda,0)<30\%$ of clear sky], as may be expected if production is not strongly limited by PAR. Water transparency to UV was also an important factor in determining the extremes of production, but the relationship was not simple. The greatest inhibition did not occur in the clearest water column, actually $K_d(325)$ was 8.7 m^{-1} for the minimum P^*_z.

To further analyze how predicted P^*_z is affected by variations in water column transparency, measures of UV (T_{PIR}) and PAR (T_{PAR}) transparency were calculated, both in units of meters. The transparency for inhibiting irradiance (T_{PIR}) was calculated using the equation of Pienitz and Vincent [9] as modified [28]

$$T_{PIR}=\sum_{\lambda=290\ nm}^{395\ nm}\frac{1}{K_d(\lambda)}\cdot\frac{\epsilon(\lambda)\cdot E(\lambda,0)}{E^*_{inh}(0)}\cdot\Delta\lambda \quad (3)$$

For the Rhode River and adjacent waters, calculated T_{PIR} for the sensitivity analysis averaged 0.15 m (Table 1). Transparency for PAR ($=1/K_{PAR}$ [9],) was 0.55 m on average. The ratio of these two transparencies (T_{PIR}/T_{PAR}, average$=0.25$) is an indicator of how water column properties mediate the competing effects of solar irradiance as both a inhibitor and source of energy for photosynthesis. Thus, the most severe inhibition of P^*_z corresponded to situations with the highest ratio, T_{PIR}/T_{PAR}. For severe inhibition this ratio was almost 0.5 compared to around 0.1 for weak inhibition. While most combinations resulted in a ratio near the mean, there were sets of conditions that resulted in distinct groups near the upper and lower extremes (Fig. 3c).

Another indicator of the relative influence of exposure and sensitivity factors on water-column production is the variation resulting from each factor. This was estimated by specifying a fixed factor level (e.g. each of the 8 BWFs) and calculating averages over all combinations of the other factors. The calculation indicated that variations in BWFs and water column transparency have the greatest influence on the relative production (P^*_z), with the range of averages about half of the overall range (Table 1). On the other hand, absolute production (P_z) is influenced more by incident irradiance and water column transparency. Variation in the BWF is the strongest influence on relative production at the surface ($P^*(0)$) and on T_{PIR}.

Column ozone ranged between 295 and 366 DU (Dobson units) during the 28-day period for which irradiance

Table 1
Variation in water-column production and related variables in the Rhode River

	P_{zpot}	P_z	P^*_z	$P^*(0)$	T_{PIR}
Average	1.17	0.98	0.84	0.39	0.15
Variation					
All (%)	±62	±65	±18	±88	±61
BWF (%)	±14	±16	±8.1	±42	±8.6
Incident irradiance (%)	±32	±28	±4.9	±50	–
Water column transparency (%)	±32	±33	±7.5	–	±53

Data are the results of a sensitivity analysis of depth integrated potential production (P_{zpot}, mg C m^{-2} h^{-1}), depth integrated production including the effect of inhibition by UV (P_z, mg C m^{-2} h^{-1}), the ratio of UV-inhibited to potential production, for the water column ($P^*_z=P_z/P_{zpot}$) and at the surface [$P^*(0)=P(0)/P_{pot}(0)$] and weighted transparency for biologically effective UV (T_{PIR}, m). Variation is quantified as the difference between maximum and minimum values relative to the overall average, results are expressed as ±half this range. 'All' refers to the range over all 3584 combinations of conditions. The variation due to each factor was estimated as range resulting when means are computed for each of the 8 BWFs, 28 surface UV spectra or 16 water-column attenuation spectra, averaged over all combinations of the other factors. Cells are empty for factors that have minimal effect on the variable.

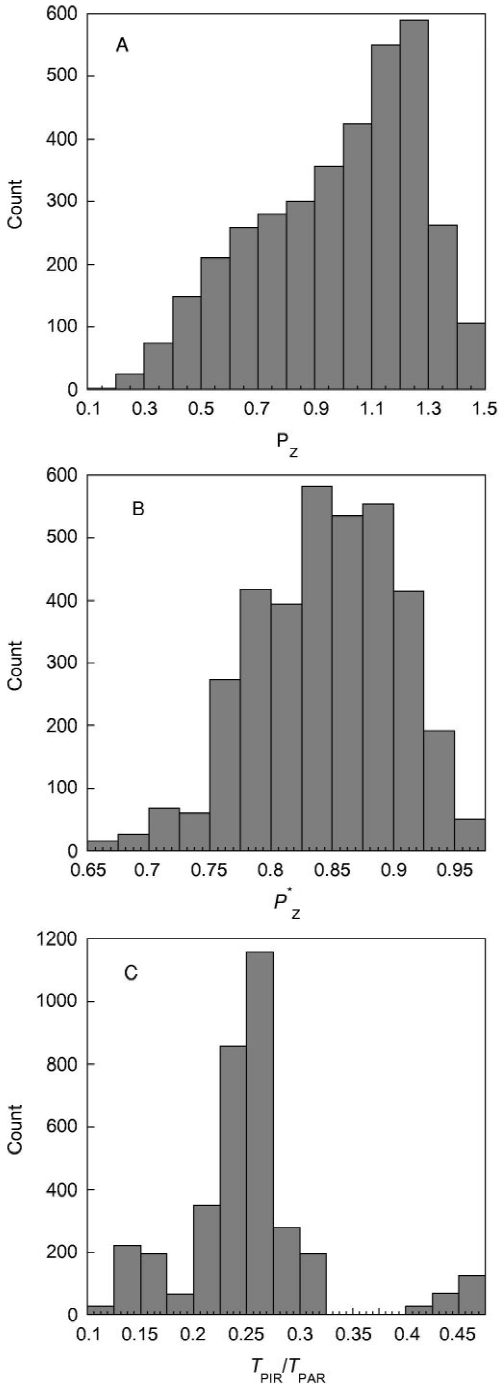

Fig. 3. Distribution of model calculated water-column production and UV/PAR transparency ratio for conditions used in the sensitivity analysis. Each histogram shows the number of instances in each category over a total of 3584 combinations. (A) Water column production (P_z, mg C m^{-2} h^{-1}) for unit Chl and maximum rate of photosynthesis, (B) water column production as a proportion of the potential production in the absence of UV inhibition (P^*_z, dimensionless), (C) ratio of transparency for biologically effective UV (T_{PIR}, m) to PAR (T_{PAR}, m).

spectra were selected. This is about a 20% variation in ozone, but there was no significant correlation between ozone and modeled P_z. A separate analysis was therefore undertaken to determine the influence of ozone, per se. A series of model irradiance curves was generated for midday, clear-sky, summer solstice conditions using parameters for June 21, 1999 as described previously, but varying total column ozone by 25 DU increments from 250 to 400 DU. A second series of production model calculations was then performed to compute surface and water column production using these spectra over all combinations of BWFs and K_d. The results indicate that ozone depletion, per se, has a small effect on production in the Rhode River, with an average of 9% drop in surface production and 1% decrease in water column production over the given range (Fig. 4). This reflects the limited transparency of the water column to UV-B [17]. Accordingly, excluding the UV-B contribution in model calculations typically increases water column production by only 3% of P_{zpot} and decreases inhibition by approximately 18% (=3%/16%). The contribution of UV-B would be even less if attenuation coefficients in the UV-B range are actually higher than the extrapolated values used in the present analysis. Thus, the decrease associated with the 20% variation of column ozone in the observed irradiance series is probably obscured by concomitant variation caused by changes in other atmospheric conditions.

The strong influence on predicted production of variation in exposure and sensitivity factors suggested that a simple relationship may exist between these factors and

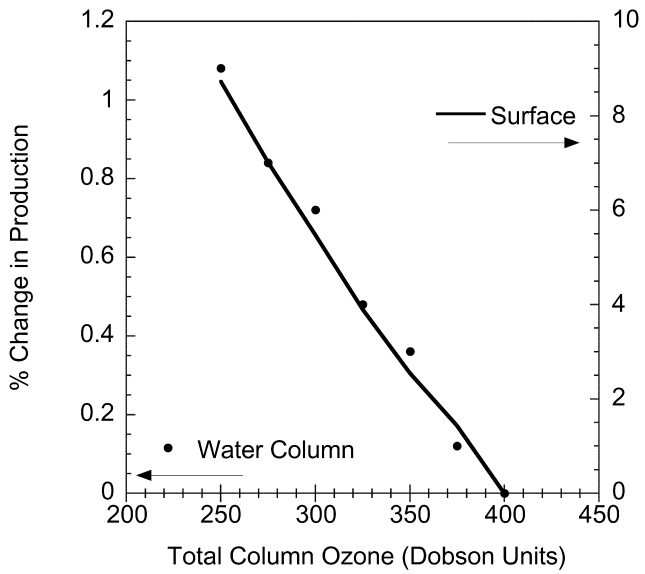

Fig. 4. Production in the Rhode River as a function of total column ozone. Surface production ($P(0)$, mg C m^{-3} h^{-1}) and water column production (P_z, mg C m^{-2} h^{-1}) were calculated for all combinations of BWFs and water column transparency using seven modeled irradiance spectra based on atmospheric conditions for June 21, 1999 but using seven levels of total column ozone ranging from 250 to 400 Dobson Units (DU), with an increment of 25 DU. Results are shown as percentage decrease in production at each ozone level in proportion to production at 400 DU, left axis (points) water column production, right axis (line) surface production.

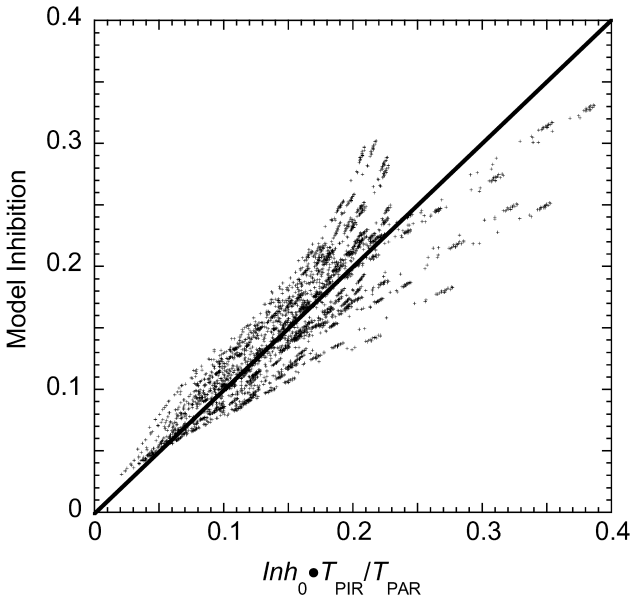

Fig. 5. Relationship between inhibition of water column production (Inh_z, dimensionless) calculated for sensitivity analysis conditions and inhibition of production as predicted by the product of surface inhibition (Inh_0) and the ratio of UV to PAR transparency ratio ($Inh_0 \cdot T_{PIR}/T_{PAR}$); diagonal line indicates a 1:1 relationship. The overall R^2 between the two variables is 0.80.

inhibition by UV (i.e. less complex than a complete numerical integration). A good agreement was found between inhibition of water column production ($Inh_z = 1 - P^*_z$) and the product of surface inhibition ($Inh_0 = 1 - P^*_0$) and the ratio of UV to PAR transparency, i.e.

$$Inh_z = Inh_0 \cdot \frac{T_{PIR}}{T_{PAR}} \quad (4)$$

This relationship reproduced model calculated inhibition with an overall R^2 of 0.80 (Fig. 5). The fidelity of the relationship to a 1:1 ratio varied according to the water optical properties. Eq. (4) slightly underestimated inhibition for the highest T_{PAR} values (0.8–1 m) and overestimated for the lowest T_{PAR} values (0.25–0.3 m). The standard error of the inhibition estimate was 2.6% of P_{zpot}.

4. Discussion

A modeling approach has been used to investigate the relative importance of exposure and sensitivity factors in determining UV inhibition of water column production during early summer conditions in a temperate estuary. The natural range of variations in sensitivity as measured by the biological weighting function for inhibition of photosynthesis and variations in transparency both significantly influenced the calculation of water column production, with each factor making an approximate equal contribution.

Inhibition of midday production in the Rhode River averaged about 16% over all combinations, considerably less than the around 25–30% inhibition of daily production calculated for the Weddell-Scotia Confluence [18] and Antarctic Peninsula waters [29]. On the other hand, the predicted inhibition of integrated production for the Rhode River is at a similar level as calculated for Lake Michigan [30] (effect of $<$370 nm only) and lakes in the Swiss Alps [14]. Interestingly, the ratio T_{PIR}/T_{PAR} in the Swiss lakes was in the same range as the Rhode River (0.2–0.4) despite the generally clearer water in the lakes. This reinforces the conclusion that the predicted effect of UV depends more on the relative penetration of UV and PAR rather than the UV transparency by itself. Thus, inhibition by UV can be significant even in a turbid estuary with high attenuation coefficient for biologically effective wavelengths, especially under conditions of simultaneous low transparency for PAR. The Rhode River is much more dynamic, optically, than the WSC, so that changes in transparency emerge as a primary factor affecting exposure in this system, whereas vertical mixing was the primary factor affecting exposure in the WSC. Indeed, fine temporal scale (1 h) monitoring of optical properties in the Rhode River has revealed many-fold variations in transparency on daily time scales [31].

In the present analysis, vertical mixing was not considered as factor since an irradiance-based model of UV response was used, consistent with measured kinetics of inhibition and recovery [17]. Strong vertical mixing could still affect production if residence times were comparable to the characteristic time scales of response to UV [18,32]. However, an irradiance based BWF/P-I model was a good predictor of water column production in a Swiss lake, even when incubations bottles were circulated during exposure [33]. The analysis also assumes that there is a homogeneous vertical distribution of phytoplankton biomass. On average, this is a good approximation to conditions in this shallow estuary. However, localized and transient deviations from homogeneity certainly do occur. In particular, dinoflagellates appear to migrate away from the surface under calm conditions. This would obviously affect the degree of UV inhibition of production.

Implementation of the BWF/P-I approach for predicting water column production requires full spectral irradiance at nanometer scale resolution. Since only the UV-B spectrum is monitored at the site, UV-A was obtained by scaling the output of a radiative transfer model. A similar procedure was used in the modeling of production in Lake Lucerne. At the Swiss site (EAWAG field station), SR18 measurements were conducted in parallel with operation of broadband sensors (Macam) for UV-B, UV-A and PAR [34]. Model spectra were also calculated using the STAR program and scaled to agree with the SR18 at 320 nm. The resultant UV-A and PAR irradiances were consistent with the independent UV-A and PAR measurements, after accounting for the respective spectral response of the sensors. Results for these two sites, together with similar efforts by

other groups [35], support the combined use of multifilter radiometers and radiative transfer models as an efficient method of obtaining spectral irradiance for use in quantitating the effects of UV with weighting functions.

The sensitivity analysis approach provides a detailed picture of how multiple influences can combine to affect ecosystem response to a primary stressor such as UV. The results of this initial analysis motivate the extension of the approach to other types of variation, such as vertical mixing and to the quantitation of UV effects on other processes, such as bacterial growth and survival. The main disadvantage of conducting a full sensitivity analysis is that it is computationally intensive. However, the results also show that a simple expression involving surface inhibition, UV and PAR transparency gives a fairly accurate estimate of water column inhibition. This expression could be used for general assessments of how variations in some parameters translate to water column effects in estuaries. For example, the expression could be used to indicate how variations in nutrient availability (e.g. nitrogen) may influence UV effects on water column, since such availability affects both phytoplankton BWFs [36] and water column optics (through controls on blooms [19]). Systematic deviations from the relationship are apparent suggesting that improvements in accuracy are possible. The deviations are related to T_{PAR} (and thus K_{PAR}), so a more consistent relationship may be obtained if PAR is estimated using spectral transmission (instead of an average K) or by using photosynthetically utilizable irradiance (PUR) as a basis for the relationship. More complex expressions utilizing PUR and other parameters have been developed which accurately predict inhibition over a wide range of optical conditions [28,37]. Future work will examine to what extent these simple approaches to assessing UV effects apply to other temperate and polar environments.

Acknowledgements

Charles Gallegos and Karen Yee are acknowledged for making available optical data from the Rhode River, which were acquired with support from Environmental Protection Agency, CISNET grant number R826943. Additional support was provided by NSF Office of Polar Programs grant OPP-9615342 and the Smithsonian Institution Scholarly Studies Program.

References

[1] O. Holm-Hansen, D. Lubin, E.W. Helbling, UVR and its effects on organisms in aquatic environments, in: A.R. Young et al. (Ed.), Environmental UV Photobiology, Plenum, New York, 1993, pp. 379–425.
[2] D.-P. Häder, The effects of ozone depletion on aquatic ecosystems. Environmental Intelligence Unit, R.G. Landes, Georgetown, TX, 1997.
[3] The effects of UV radiation on marine ecosystems, in: S.J. de Mora, S. Demers, M. Vernet (Eds.), Environmental Chemistry Series, Cambridge University Press, Cambridge, 2000.
[4] D. Lubin, E.H. Jensen, Effects of clouds and stratospheric ozone depletion on ultraviolet radiation trends, Nature 377 (1995) 710.
[5] S. Madronich, G.J.M. Velders, Halocarbon scenarios for the future ozone layer and related consequences, in: C.A. Ennis (Ed.), Scientific Assessment of Ozone Depletion, World Meterological Organization, Geneva, 1998, pp. 1111–1138.
[6] J.J. Cullen, P.J. Neale, M.P. Lesser, Biological weighting function for the inhibition of phytoplankton photosynthesis by ultraviolet radiation, Science 258 (1992) 646–650.
[7] H. Maske, Daylight ultraviolet radiation and the photoinhibition of phytoplankton carbon uptake, J. Plankton Res. 6 (1984) 351–357.
[8] D.W. Schindler, P.J. Curtis, B. Parker, M.P. Stainton, Consequences of climate warming and lake acidification for UV-B penetration in North American boreal lakes, Nature 379 (1996) 705–708.
[9] R. Pienitz, W.F. Vincent, Effect of climate change relative to ozone depletion on UV exposure in subarctic lakes, Nature 404 (2000) 484–487.
[10] P.R. Leavitt, R.D. Vinebrooke, D.B. Donald, J.P. Smol, D.W. Schindler, Past ultraviolet radiation environments in lakes derived from fossil pigments, Nature 388 (1997) 457–459.
[11] J. Herman, R.L. McKenzie, Ultraviolet radiation at the earth's surface, in: C.A. Ennis (Ed.), Scientific Assessment of Ozone Depletion: 1998, World Meteorological Organization, Geneva, 1999, pp. 91–944.
[12] P.J. Neale, M.P. Lesser, J.J. Cullen, Effects of ultraviolet radiation on the photosynthesis of phytoplankton in the vicinity of McMurdo station (78°S), in: C.S. Weiler, P.A. Penhale (Eds.), Ultraviolet Radiation in Antarctica: Measurements and Biological Effects, Am. Geophysical Union, Washington, DC, 1994, pp. 125–142.
[13] M.P. Lesser, P.J. Neale, J.J. Cullen, Acclimation of Antarctic phytoplankton to ultraviolet radiation: ultraviolet-absorbing compounds and carbon fixation, Molec. Mar. Biol. Biotech. 5 (1996) 314–325.
[14] P.J. Neale et al. Quantifying the response of phytoplankton photosynthesis to ultraviolet radiation: Biological weighting functions versus in situ measurements in two Swiss lakes, Aquatic Sci. 63 (2001) in press.
[15] P.J. Neale, A.T. Banaszak, C.R. Jarriel, Ultraviolet sunscreens in dinoflagellates: mycosporine-like amino acids protect against inhibition of photosynthesis, J. Phycol. 34 (1998) 928–938.
[16] P.J. Neale, J.J. Cullen, R.F. Davis, Inhibition of marine photosynthesis by ultraviolet radiation: variable sensitivity of phytoplankton in the Weddell-Scotia Sea during the austral spring, Limnol. Oceanogr. 43 (1998) 433–448.
[17] A.T. Banaszak, P.J. Neale, UV Sensitivity of photosynthesis in phytoplankton from an estuarine environment, Limnol. Oceanogr. 46 (2001) 592–600.
[18] P.J. Neale, R.F. Davis, J.J. Cullen, Interactive effects of ozone depletion and vertical mixing on photosynthesis of Antarctic phytoplankton, Nature 392 (1998) 585–589.
[19] C.L. Gallegos, T.E. Jordan, D.L. Correll, Event-scale response of phytoplankton to watershed inputs in a subestuary: timing, magnitude and location of blooms, Limnol. Oceanogr. 37 (1992) 813–828.
[20] D.L. Correll, C.O. Clark, B. Goldberg, V.R. Goodrich, D.R. Hayes Jr., W.H. Klein, W.D. Schecher, Spectral ultraviolet-B radiation fluxes at the earth's surface: long-term variations at 39°N, 77°W, J. Geophys. Res. 97 (1992) 7579–7591.
[21] C.L. Gallegos, K. Yee, D. Sparks, Unpublished spectral irradiance data for the Rhode River, 2000.
[22] T.E. Jordan, D.L. Correll, J. Miklas, D.E. Weller, Nutrients and chlorophyll at the interface of a watershed and an estuary, Limnol. Oceanogr. 36 (1991) 251–267.

[23] E. Early et al., The 1995 North American interagency intercomparison of ultraviolet monitoring spectroradiometers, J. Res. Natl. Inst. Stand. Technol. 103 (1998) 15–62.
[24] A. Ruggaber, R. Dlugi, T. Nakajima, Modeling of radiation quantities and photolysis frequencies in the troposphere, J. Atmos. Chem. 18 (1994) 171–210.
[25] J.J. Cullen, P.J. Neale, Biological weighting functions for describing the effects of ultraviolet radiation on aquatic systems, in: D.-P. Häder (Ed.), Effects of Ozone Depletion On Aquatic Ecosystems, R.G. Landes, Austin, 1997, pp. 97–118.
[26] A.D. Jassby, T. Platt, Mathematical formulation of the relationship between photosynthesis and light for phytoplankton, Limnol. Oceanogr. 21 (1976) 540–547.
[27] S. Markager, W.F. Vincent, Spectral light attenuation and the absorption of UV and blue light in natural waters, Limnol. Oceanogr. 45 (2000) 642–650.
[28] J.J. Cullen, R.F. Davis, Y. Huot, M.K. Lehmann, Quantifying effects of ultraviolet radiation in surface waters, in: G.D. Gilbert, R.J. Frouin (Eds.), Ocean Optics: Remote Sensing and Underwater Imaging, 2001.
[29] N.P. Boucher, B.B. Prézelin, Spectral modeling of UV inhibition of in situ Antarctic primary production using a field derived biological weighting function, Photochem. Photobiol. 64 (1996) 407–418.
[30] W.R. Gala, J.P. Giesy, Effects of ultraviolet radiation on the primary production of natural phytoplankton assemblages in Lake Michigan, Ecotoxicol. Environ. Safety 22 (1991) 345–361.
[31] C.L. Gallegos, P.J. Neale, unpublished data (2000).
[32] E.W. Helbling, V. Villafañe, O. Holm-Hansen, Effects of ultraviolet radiation on Antarctic marine phytoplankton photosynthesis with particular attention to the influence of mixing, in: C.S. Weiler, P.A. Penhale (Eds.), Ultraviolet Radiation and Biological Research in Antarctica, American Geophysical Union, Washington, DC, 1994, pp. 207–227.
[33] J. Köhler, M. Schmitt, H. Krumbeck, M. Kapfer, E. Litchman, P.J. Neale, Effects of UV on carbon assimilation of phytoplankton in a mixed water column, Aquatic Sci. 63 (2001) in press.
[34] P.J. Neale, P. Bossard, Y. Huot, Incident and in situ irradiance in Lakes Cadagno and Lucerne: a comparison of methods and models, Aquatic Sci. 63 (2001) in press.
[35] J.T.O. Kirk et al., Measurements of UV-B radiation in two freshwater lakes: an instrument intercomparison, Arch. Hydrobiol. Beih Ergebn. Limnol. 43 (1994) 71–99.
[36] E. Litchman, P.J. Neale, A.T. Banaszak, Increased sensitivity to ultraviolet radiation in nitrogen-limited dinoflagellates: photoprotection and repair, Limnol. Oceanogr. (2001) accepted for publication.
[37] M.K. Lehmann, R.F. Davis, Y. Huot, J.J. Cullen, Biologically weighted transparency: a predictor for water column photosynthesis and its inhibition by ultraviolet radiation, Limnol. Oceanogr. (2001) submitted for publication.